Applications of Geospatial Technologies and Frequency Ratio Method in Groundwater Potential Mapping in Iyenda River Catchment, Konso Area, Rift Valley, Ethiopia

Muralitharan Jothimani, Abel Abebe, and Gosaye Berhanu

Abstract The present study aimed to map the potential groundwater zones in the Iyenda river catchment, Konso area, Rift Valley, Ethiopia. The potential groundwater zones were defined in this study using a frequency ratio (FR) model. The following nine thematic layers were considered in the present study, such as lithology, lineament density, slope, drainage density, land use/land cover (LULC), topographic wetness index (TWI), normalized difference vegetation index (NDVI), drainage density, rainfall, and soil types. The above-mentioned thematic layers were prepared using primary and satellite data in the ArcGIS software environment. During fieldwork, thirty-four water points, including deep bore wells, springs, and hand pump locations, were collected using GPS. In the FR model, 24 well points were used to calculate the success rate, and the rest ten well points were used to calculate the prediction rate. Groundwater prospect zones were further categorized into three groups: very good, moderate, and very low. Low groundwater prospective zones account for 39.23% of the current study, whereas medium and high potential groundwater zones account for 38.33 and 22.44%. The area under curve (AUC) technique was used to examine the accuracy of the potential groundwater zones. The AUC value for the success rate prediction rate is 0.735 and 0.732, respectively, and the same indicates the model produces excellent results in the current study. The findings of this study may aid in effective water resources management in the present study area, allowing planners and decision-makers to design suitable groundwater development plans for a sustainable environment.

Keywords Groundwater potential · Geospatial · Frequency ratio · Iyenda catchment · Konso area · Ethiopia

M. Jothimani (✉) · A. Abebe · G. Berhanu
Department of Geology, Arba Minch University, Arba Minch, Ethiopia
e-mail: muralitharangeo@gmail.com

1 Introduction

Groundwater is one of the world's most essential and renewable natural resources. In many places globally, groundwater is extensively used for household, commercial, and agricultural purposes [1]. The reliance on groundwater is increasing all the time. These rising demands frequently lead to overexploitation, putting a considerable strain on this finite freshwater supply [2, 3]. The water table has been steadily declining as a result of groundwater exploitation [4].

Furthermore, owing to inappropriate irrigation patterns, dense population, and climatic change, groundwater problems have intensified, primarily in many parts of the world [5]. Ethiopia has had tremendous economic growth, including an average yearly growth rate of 8%; from 1998 to 2016, the pace of urbanization expanded by 10%, resulting in fast urbanization rates ranging from 6 to 20%. This expansion has resulted in uncontrolled migration from rural areas to major urban centers searching for work, significantly impacting current infrastructures, especially water supply [6]. Ethiopia is known as East Africa's "water tower". However, water is frequently unavailable when it is needed due to considerable temporal and geographical fluctuations in rainfall and complicated aquifers. Ethiopia's groundwater contributes little to its agricultural growth [7].

Groundwater sources like bore wells, springs, and shallow wells provide domestic water to most Ethiopian towns and villages. Groundwater accounts for more than 70% of Ethiopia's water supply [8]. Despite this, just 34% of the population has access to safe drinking water. It implies that groundwater development and use must be in great demand in the country. But there is an absence of comprehensive knowledge about Ethiopia's groundwater potential. And there is a significant gap in estimating groundwater reserves in Ethiopia [8]. In Ethiopia, several complex variables hinder the efficient and effective use of groundwater. The most critical is the absence of accurate hydrological data, a lack of comprehension of aquifer architecture and features, and technical constraints [9].

As a result, it is vital to comprehend the structure of aquifers and explore cost-effective, comprehensive, and user-friendly methodologies and processes for groundwater detection, extraction, and monitoring [9]. Ethiopia's aquifers are very intricate, low-storage aquifers that are segregated. The complex geological nature is to account for this. As a result, conventional groundwater investigation methods in Ethiopia will be time-consuming and costly [10]. Groundwater is underutilized in Ethiopia due to increased development and operating costs and a failure to understand groundwater dynamics [11]. In Ethiopia, groundwater is mainly used for domestic purposes. There have been a few instances of groundwater being utilized for farming and other non-domestic purposes. There has been minimal research on groundwater potentiality for agriculture and other non-domestic purposes [12]. There are very few regional studies on geospatial technologies in Ethiopia to delineate groundwater potential [10].

Various elements, such as geology, soil, geological structures, land use/land cover (LULC), topography, and rainfall, influence groundwater occurrence. It is easier

to predict a region's groundwater potential using various techniques considering all of these elements [13]. Before a groundwater borehole can be dug or drilled, several approaches such as geophysical, hydrogeological, geological, and spatial methods have been employed to analyze a suitable location for groundwater potential. Furthermore, several of these approaches are too costly and challenging to implement. However, spatial technology has aided in developing a method for groundwater investigations [14, 15]. Satellite images are utilized to create the following layers: lithology, landscapes, LULC, stream, slope, Normalized Difference Vegetation Index (NDVI), Topographic Wetness Index (TWI), geological structures, and so on, which serve as the basis for determining the potential groundwater zone [16].

The following researchers from across the world, including Ethiopia, employed remote sensing (RS) and Geographic Information System (GIS) technology to delineate prospective groundwater zones, including in Karur district, Tamil Nadu, India, by using AHP methods [17]; in the Leylia–Keynow watershed, southwest of Iran [18]; in Tirunelveli Taluk, South Tamil Nadu, India [19]; in Guna tana landscape, upper Blue Nile Basin, Ethiopia [20]; and Jemma River basin, Ethiopia [10]. Various scholars have used different models in potential groundwater mapping worldwide, such as the logistic regression model [21], multi-criteria decision evaluation [22, 23], random forest model [24, 25], evidential belief function [24], frequency ratio [26–28], weights of evidence model [29, 30], and drainage morphometric analysis [31, 32].

With this background, using remote sensing data, GIS technologies, and a probability-based frequency ratio technique, the current research aims to map the possible groundwater zones in the Iyenda river catchment, Konso area, Southern Ethiopia. The frequency ratio (FR) method is a data-driven framework and bivariate statistical technique for assigning rating (r) values to each class through the computation of spatial links among dependent variables (springs and wells) and the independent variable (thematic layers). In this present study, nine significant factors were taken into account, including lithology, lineament density, drainage density, Slope, NDVI, TWI, LULC, and rainfall. So far, no study has been conducted using this method and data sets in the present study area. The current study results may be helpful for researchers to carry out further research, planners, and administrators for locating suitable sites for drilling water wells.

2 Materials and Methods

2.1 Study Area

The present study area, the Iyenda river catchment, is situated in Southern Nations, Nationalities, and People (SNNPR) regional state, Rift Valley, Ethiopia. It is located geographically between 37° 15′ 28″ and 37° 35′ 15″ E longitude and 5° 18′ 28″ to 5° 39′ 29″ N latitude. The present study area covers a total area of 576 km^2. Gidole,

Gato, and Konso are the significant settlements. Figure 1 shows the location map of the present study area. The study area has rugged topography and elevation ranging between 1055 and 2576 m, and the terrain slope is between 0° and 51° (Fig. 2). The
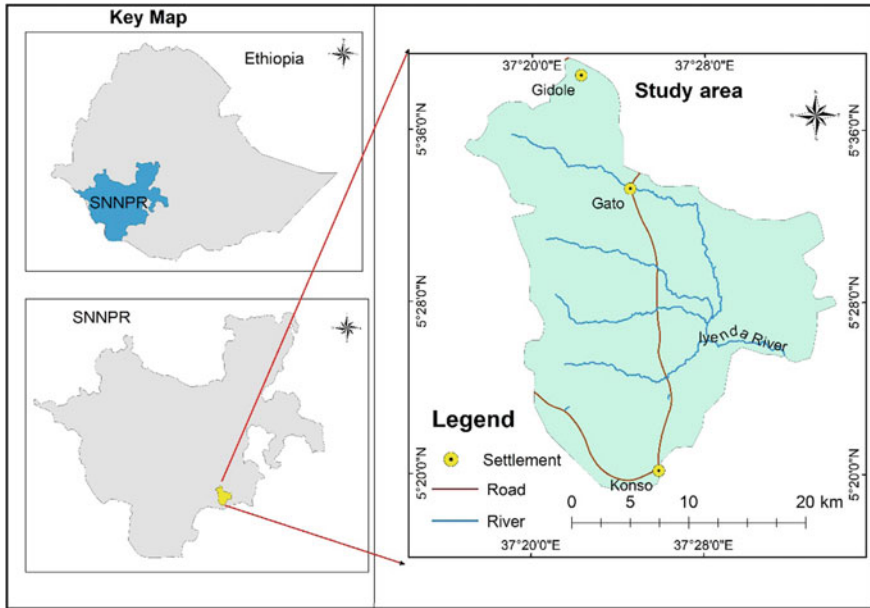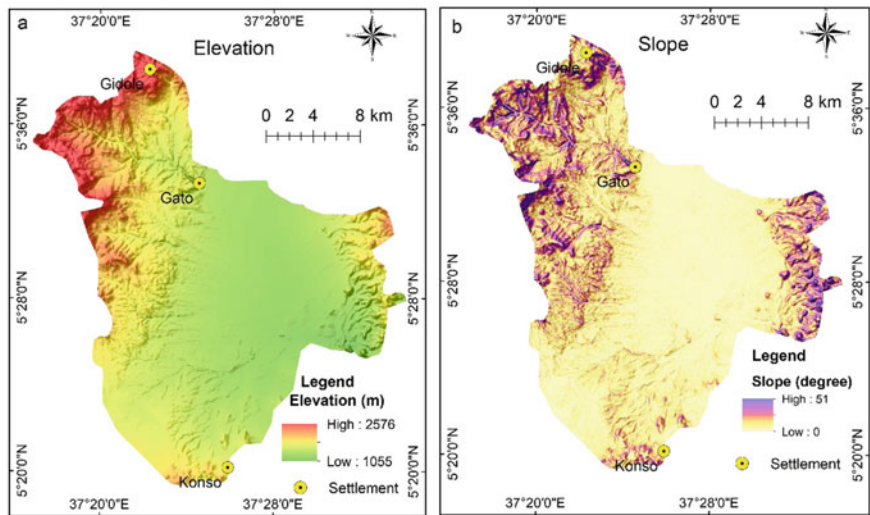

Fig. 1 Study area

Fig. 2 Topography and slope map

present study area's northwest and southwest rift margins have a higher elevation, rugged topography, steep slope in the current location, and vice versa in the rift floor, which divided rift margins.

2.2 Data Collection and Preparation of Thematic Layers

The present study aims to use remote sensing data, GIS tools, and the frequency ratio approach to identify possible groundwater zones in Ethiopia's Iyenda river watershed. The methodology flow chart for the present study is shown in Fig. 3. The multiple thematic layers were produced by utilizing several data sets, including remote sensing data, secondary information, and field observations, to carry out the present study. The ArcGIS 10.8 software's many features were used to prepare thematic layers and conduct data analysis. The WGS-84, UTM-37 N projection system was used to project all of the data sets. The data and sources utilized in this investigation are listed in Table 1.
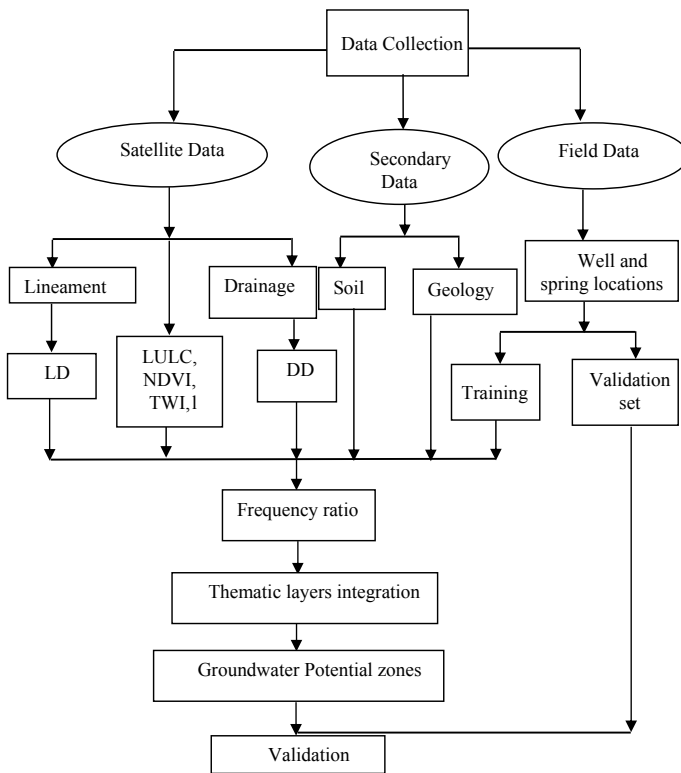

Fig. 3 Methodology flow chart

Table 1 Input data and its sources

S.No.	Thematic layer	Data	Data source
1	Geology	Geological map of Ethiopia, Landsat-8 OLI (30 m spatial resolution)	Geological Survey of Ethiopia, https://earthexplorer.usgs.gov/
2	Elevation and slope	SRTM-DEM (30 m spatial resolution)	https://earthexplorer.usgs.gov
3	Lineament	Landsat-8 OLI (30 m spatial resolution)	https://earthexplorer.usgs.gov
4	Soil	Shape file	Food and Agriculture Organization
5	Drainage	Toposheets, SRTM-DEM	Ethiopian Mapping Agency, https://earthexplorer.usgs.gov
6	Topographic wetness index	SRTM-DEM	https://earthexplorer.usgs.gov
7	Rainfall	Grid	https://chrsdata.eng.uci.edu/
8	Well/Spring locations	GPS reading	Field work
9	NDVI	Landsat-8 OLI (30 m spatial resolution)	https://earthexplorer.usgs.gov

2.3 Thematic Layers Preparation

The following thematic layers were used, such as lithology, lineament density, slope, TWI, soil, rainfall, drainage density, LULC, and NDVI in the present study. Lithology is recognized as one of the most significant markers of hydrogeological character-istics since it affects aquifer materials' permeability and porosity [33]. Initially, the lithological contact of the present study area was demarcated using a Geological map prepared by the Ethiopian Geological Survey. Hornblende gneiss, basalt, and alluvial deposits are the central rock units present in the study area. The above-mentioned rock units were further classified based on their weathering nature. And the same was identified using false-color composite of the Landsat-8 OLI satellite image. The rift margins comprise the differently weathered basalts and hornblende gneiss, and alluvial deposits cover the rift floor (Fig. 4b).

In hard rock fractured aquifer areas, lineaments regulate groundwater ingress and serve as a transmission medium [34]. The present research area lineaments were identified and extracted from a Landsat-8 OLI satellite image through a visual interpretation approach based on the image's tonal contrast. Further, the lineaments were extracted in the satellite data, where the linear drainages with moisture content appeared as black tonal contrast. The lineament density (km/km^2) map was created with ArcGIS software's line density tool, and the same were classified into five classes natural break method viz (0–0.25, 0.26–0.51, 0.52–0.77, 0.78–1.03, and 1.04–1.29). The present study area's lineament density map is shown in Fig. 4a.
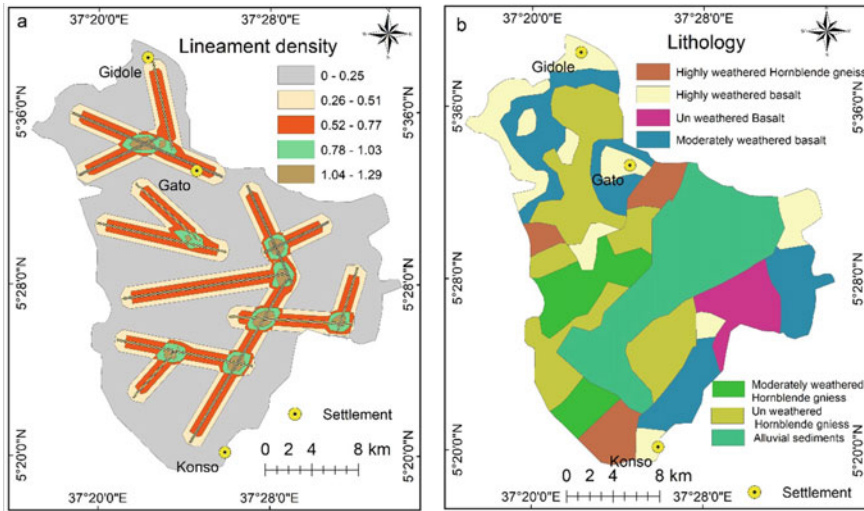
Fig. 4 Lineament density and lithology map

In general, water moves slowly over moderate slopes, allowing for more significant infiltration into the substrate. The present study area's slope map research region was created using ArcGIS 9.3's Spatial Analysis tools and a DEM. On the other hand, the steep slope increased run-off and decreased infiltration into the surface [35]. SRTM-DEM with 30 m spatial resolution data was used to prepare the slope layer of the present study area. The minimum and maximum slope of the current study area are 00 and 540, respectively. Using ArcGIS software's natural break technique, the slope layer has been further categorized into five groups (0–4.66, 4.67–9.74, 9.75–16.03, 16.04–23.94, and 23.95–51.74). Figure 2b shows the slope map of the present study area, and it has been observed that the rift margins have a steep slope compared to the rift floor.

Drainage density, which negatively correlates to soil and rock permeability, is an important indicator in evaluating the potential groundwater zones. High drainage density levels cause run-off and thus indicate a limited groundwater occurrence. In contrast, if lineaments or fractures control the drainage system of any area, then high drainage density areas are potential for groundwater occurrences [28]. The present study area's drainage system is controlled by structural features [32]. SRTM-DEM data and Archydro toolset of ArcGIS software were used to automatically extract the present study area's drainage, as procedures suggested by Maidment [36]. The drainage density (km/km^2) map was created with ArcGIS software's line density tool, and the same was classified into five classes natural break method viz (0–0.42, 0.42–0.84, 0.85–1.26, 1.27–1.68, and 1.69–2.10). The drainage density map for the current study area is given in Fig. 5a.

The LULC of a particular region has a significant impact on groundwater occurrence [37]. Surface run-off and flooding are more in the built-up areas, primarily
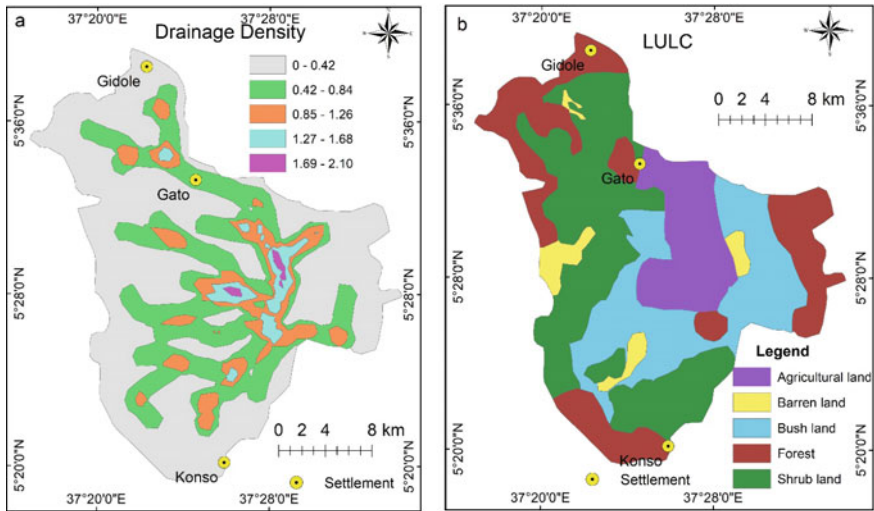
Fig. 5 Drainage density and LULC map

made up of impervious surfaces. On the other hand, agricultural areas are less prone to flood due to the positive relationship between vegetation density and infiltration capacity [38]. The LULC map in this study was created using a false-color composite of the Landsat-8 (OLI) image. Based on the fieldwork, the LULC of the current study area was classified through visual interpretation.

The agricultural field was identified based on the FCC satellite image's rectangle shape, color, and texture [39]. The built-up land has pale bluish-white, fine texture, and uniform shape and size [40]. Forest areas were dark reddish with a fine to medium texture and irregular and varied in size. Barren land was generally identified by its light to dark blue tone and gritty texture [41]. The primary LULC types in the study area are farm and bushland, forest, shrubland, and barren land. The forest is covered in the higher elevation in the rift margins where the rainfall is high, and shrubland is also covered significantly in the rift margins. The present study area's LULC map is shown in Fig. 5b.

The amount of rain that occurs significantly affects groundwater recharge in any region [28]. In the present study, rainfall data in the grid format for the year 2000–2020 was downloaded from the PERSIANN (Precipitation Estimation from Remotely Sensed Information using Artificial Neural Networks) developed by the Center for Hydrometeorology and Remote Sensing (CHRS) at the University of California, Irvine (UCI). The weblink for downloading the rainfall data is https://chrsdata.eng.uci.edu/. For twenty years (2001–2020), average rainfall data was downloaded as a grid format with a spatial resolution of 4 km × 4 km. The minimum and maximum rainfall of the present study area are 521 mm and 623 mm, respectively. The same was classified into five categories, as shown in Fig. 6a.
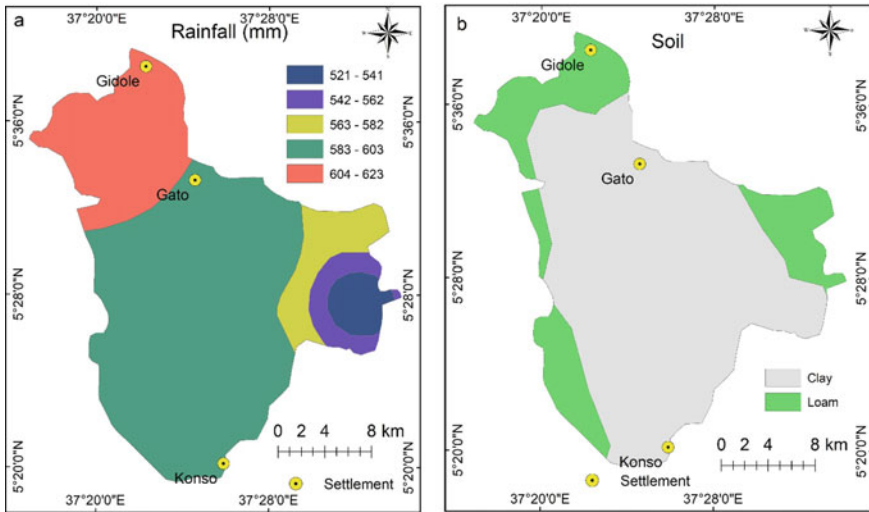
Fig. 6 Rainfall and soil map

The type of soil has a vital role in determining possible groundwater zones. Soil mapping often entails identifying soil types with distinguishable features. The soil data for the current research area was retrieved from the Food and Agriculture Organization [42]. The present study area covered clay (76%) and loam (24%) majorly. A soil map is shown in Fig. 6b.

The examination of the normalized difference vegetation index (NDVI) is considered as an approximate estimate of the quantity of vegetation present and the potential for groundwater across a given area [43]. The NDVI of the present location was calculated using the following Eq. (1).

$$NDVI = (Near infrared - Red)/(Red + Near\text{-}infrared) \qquad (1)$$

In this study, the NDVI was calculated using ArcGIS software's raster calculator. -0.15 and 0.44 are the minimum and maximum NDVI values further, classified into three categories. The maximum values were observed where forest and bushland have occurred. In contrast, negative or minimum values were found around the settlement and barren land. Figure 7a shows the NDVI map.

The topographic wetness index (TWI) evaluates the hydrologic process' topographic control. TWI is a metric that assesses the potential of wetlands. Wetland potential is shown in areas with a high positive TWI value. The zones show the erosion potential with a low TWI value [44]. The SRTM-DEM and TWI tool in QGIS 3.18 software were used to prepare the TWI for the present study. The minimum and maximum TWI values for the current study are 3.59 and 21.84, respectively. The same was classified into three categories Fig. 7b. The rift floor and drainages have medium and high TWI values, respectively.
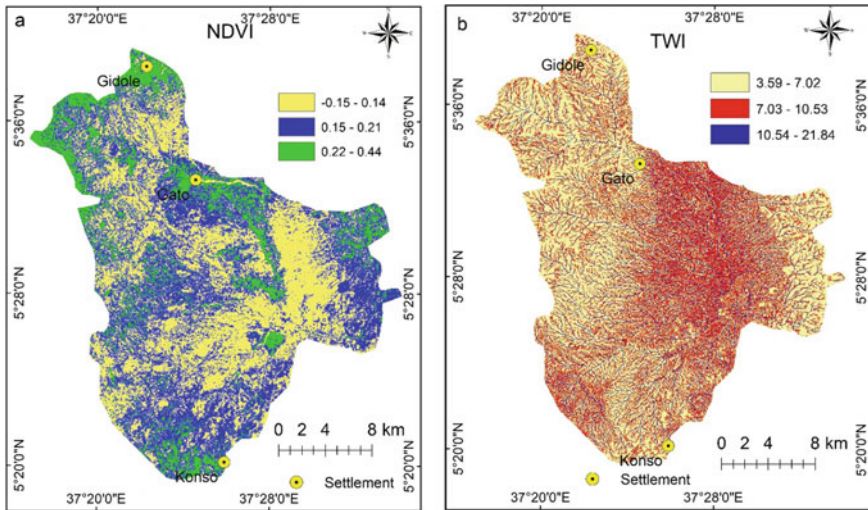
Fig. 7 NDVI and TWI map

Thirty-four well locations were located using GPS during fieldwork. Among these, 15 are springs and the remaining 12 and 7 are hand pumps and deep boreholes, respectively. Figure 8 shows the spatial distribution of springs, deep boreholes, and springs in the present study area. Seventy per cent (24 wells) of the 34 sample locations were chosen as training data sets for utilizing the FR model to map possible groundwater zoning. The remaining 30% of the samples (10 wells) were utilized for model validation.

2.4 Frequency Ratio Model and Identification of Potential Groundwater Zone

The frequency ratio (FR) method is a bivariate statistical technique widely used to establish the probability relationships among the dependent and independent variables in geospatial assessments [45]. The method examines the statistical connection between borehole locations and the factors that influence the occurrence of groundwater. In practice, the FR was computed using the following Eq. (2).

$$FR = (A/B)/(C/D) \tag{2}$$

where *A*—the number of training wells/springs in the particular sub-thematic feature, *B*—the total number of wells/springs in the study area, *C*—the number of pixels in the sub-thematic class, and *D*—the total number of sub-thematic class's pixels in the study area.
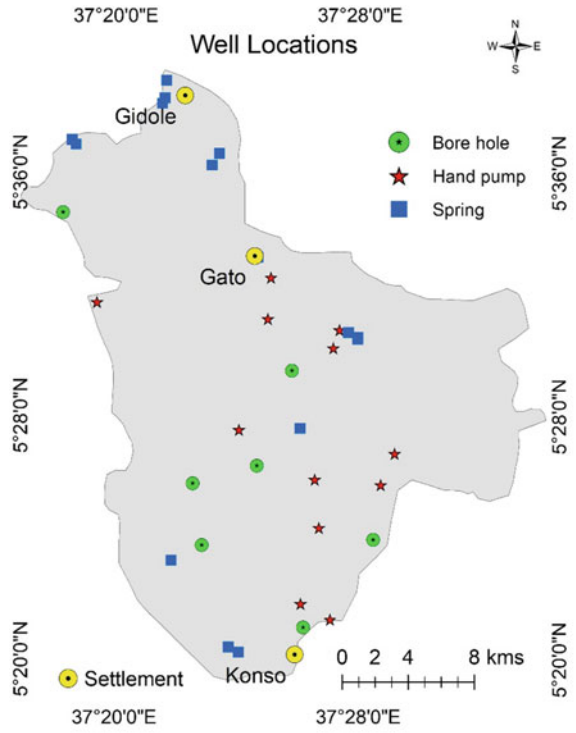
Fig. 8 Well locations map

Table 2 shows the entire weight determination computation for individual parameters. The probability of groundwater in a specific pixel may be calculated by adding the pixel values in the ArcGIS software as per Eq. (3):

$$GWPI = \sum Li_{fr} + Ld_{fr} + Sl_{fr} + Dd_{fr} + Lulc_{fr} + NDVI_{fr} + Twi_{fr} + Rf_{fr} + So_{fr}$$

$$(3)$$

where GWPI—groundwater potential index, fr—frequency ratio, Li—lithology, Ld—lineament density, Sl—slope, Dd—drainage density, Lulc—land use/land cover, NDVI—normalized difference vegetation index, Twi—topographic wetness index, Rf—rainfall, and So—soil.

Table 2 Frequency ratio calculation for potential groundwater mapping

Factor	Number of pixels	Domain percentage	No. of wells	Percentage of well	FR
Lithology					
Highly weathered hornblende gneiss	42,585	6.65	3	12.50	1.88
Moderately weathered hornblende gneiss	57,665	9.84	0	0.00	0.00
Un weathered hornblende gneiss	148,249	23.16	4	16.67	0.72
Highly weathered basalt	89,091	13.92	6	25.00	1.80
Moderately weathered basalt	113,973	17.81	3	12.50	0.0.70
Un weathered basalt	35,395	5.53	1	4.17	0.75
Alluvial sediments	153,155	23.09	7	29.17	1.26
Lineament density (km/km^2)					
0–0.25	398,590	62.27	15	62.50	1.00
0.26–0.51	103,071	16.1	4	16.67	1.04
0.52–0.77	107,617	16.81	5	20.83	1.24
0.78–1.03	19,139	2.99	0	0	0
1.04–1.29	11,696	1.83	0	0	0
Slope in degrees					
0–4.66	263,378	41.4	14	58.33	1.41
4.67–9.74	173,792	27.32	6	25.00	0.92
9.75–16.03	111,475	17.52	3	12.50	0.71
16.04–3.94	61,061	9.6	1	4.17	0.43
23.95–1.74	26,537	4.17	0	0	0
Drainage density (km/km^2)					
0–0.42	383,291	59.88	12	50.00	0.84
0.43–0.84	174,215	27.22	6	25.00	0.92
0.85–1.26	60,213	9.41	5	20.83	2.21
1.27–1.68	19,867	3.1	1	4.17	1.34

Table 2 (continued)

Factor	Number of pixels	Domain percentage	No. of wells	Percentage of well	FR
1.69–2.10	2527	0.39	0	0	0
LULC					
Agricultural land	87,181	13.62	6	25	1.84
Bush land	152,396	23.81	6	25	1.05
Forest	154,648	24.16	6	25	1.03
Shrub land	218,678	34.16	6	25	0.73
Barren land	27,210	4.25	0	0	0
NDVI					
−0.15–0.14	248,831	38.87	9	37.5	0.96
0.15–0.21	293,080	45.79	6	25	0.54
0.22–0.44	98,202	15.34	9	37.5	2.44
TWI					
3.59–7.02	395,669	62.3	13	54.16	0.86
7.03–10.53	193,179	30.42	7	29.17	0.95
10.54–1.84	46,274	7.29	4	16.67	2.28
Rainfall (mm)					
521–541	24,633	3.85	0	0	0
542–562	26,350	4.12	0	0	0
563–582	49,841	7.79	1	4.17	0.53
583–603	403,351	63.01	17	70.83	1.12
604–623	135,938	21.24	6	25	1.17
Soil					
Loam	153,450	23.97	6	25	1.04
Clay	486,663	76.03	18	75	0.98

3 Results and Discussions

3.1 Analysis of the Relationship Between Frequency Ratio and Thematic Layers

Frequency ratio values were computed for each selected thematic layer based on the association with observed well and spring locations. The frequency ratio between lithology and observed well and spring locations shows that highly weathered Hornblende gneiss and weathered basalt have a high-frequency value of 1.88 and 1.80 respectively, compared to other lithological features. The high-frequency ratio value of 1.24 was found where the lineament density value is 0.52–0.77 km/km^2. The

frequency value is decreasing when the slope angle is increasing. The association between high-frequency value and drainage density indicates that high-frequency value is concentrated where medium and high drainage density occurs in the present study area. The frequency value is high where agricultural land is present and zero in the barren land LULC classes. The high-frequency ratio value of 2.44 is observed in the high NDVI and vice versa in the low NDVI. The high-frequency ratio value of 2.28 is found where the high topographic wetness index (10.54–21.84) is observed. The inverse relationship was observed between rainfall and the frequency ratio values. Table 2 displays the frequency ratio value of various thematic layers and categories.

3.2   Groundwater Potential Assessment

The frequency ratio values for the present study ranged between 5.34 and 14.77, and the same was classified into three potential groundwater categories such as high (5.34–8.37), medium (8.38–10.11), and high (10.12–14.77). 39.23% of the present study covers the low groundwater potential zones, and 38.33% and 22.44% are the medium and high groundwater potential zones, respectively. Figure 9 shows the groundwater potential map of the present study area. It is observed from the

Fig. 9 Groundwater potential map
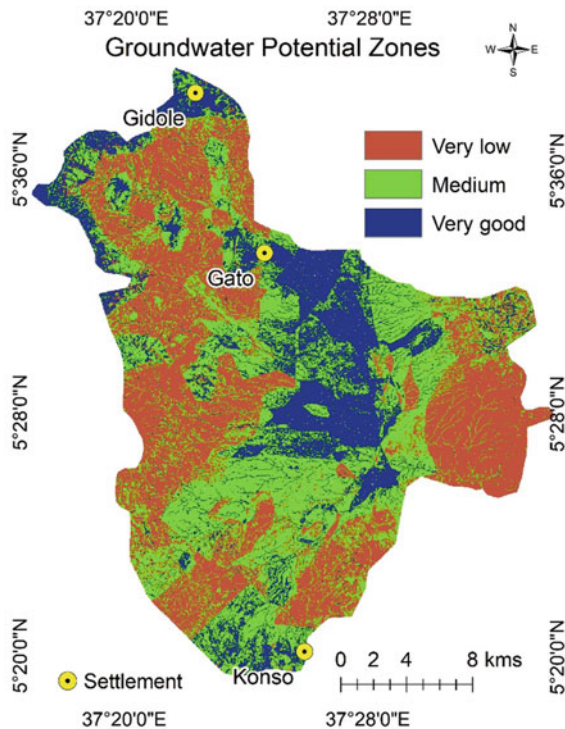
groundwater potential map that the majority of the groundwater high potential zones have occurred in the central part, and that is the rift floor and Gidole area where the plateau is present with high rainfall. Generally, the high and medium groundwater potential zones occurred where lithologically the study area covers highly weathered hornblende gneiss, weathered basalt, and alluvial deposits. And further, the results show that high and medium groundwater zones were found where medium lineament density, medium to high drainage density, less slope, high NDVI, rainfall and TWI, and loam soil occur in the present study area. In contrast, the low groundwater potential zones occurred where barren rock, high slope, less rainfall, unweathered rock, less TWI, and NDVI were found in the present study area.

3.3 Model Validation

Validation is recognized as a crucial phase in the modeling process because of its scientific significance. The receiver operating characteristics (ROC) curve technique is a widely accepted method to validate the groundwater potential mapping's results [46]. The area under curve (AUC) values range from 0.5 to 1.0, with a number around 1.0 suggesting the highest level of precision and a value around 0.5 showing the model's unreliability [24]. It has been categorized into the following categories based on the link between AUC value and prediction accuracy, excellent (0.9–1.0), very good (8–0.9), good (0.7–0.8), average (0.6–0.7), and poor (0.5–0.6) [24].

The success and prediction rate curves in this investigation were calculated using the AUC technique. The success rate was assessed at 0.735, utilizing the AUC values obtained using a training set of 24 springs, hand pumps, and bore wells to measure the success rate curve (Fig. 10). However, because the success rate is estimated using the same training data set used to create the groundwater potential zone model, it is not an acceptable approach for assessing a model's prediction capacity [25]. Consequently,
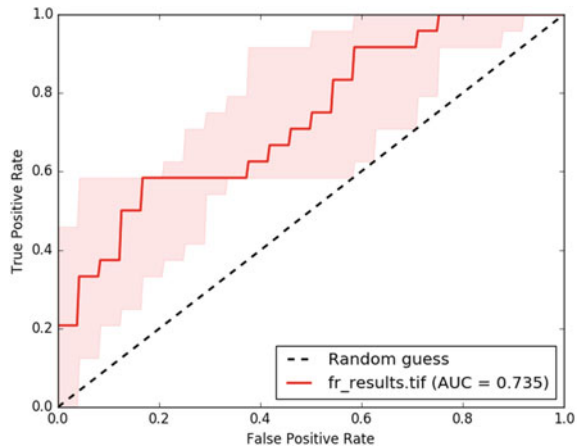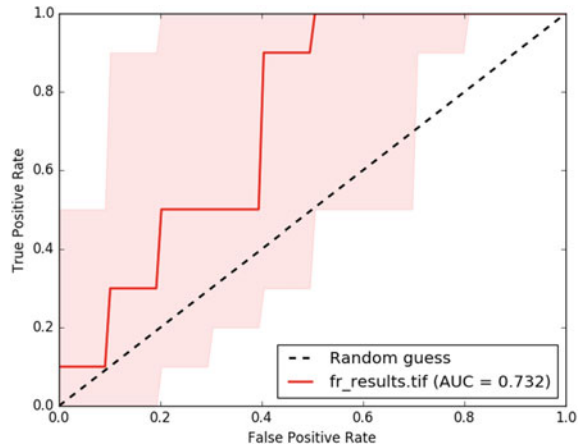
Fig. 10 Success rate curve

Fig. 11 Predication rate curve

the prediction rate curve was calculated using ten well locations not included in the frequency ratio model used to produce groundwater potential zone mapping. The AUC of the prediction rate curve is 0.732. (Fig. 11). The present AUC analysis has proven that the present model had excellent results.

4 Conclusions

Groundwater potential zone mapping is a prominent field of study, particularly in dry and semi-arid environments. Globally, many approaches for assessing regional groundwater potential have been used. Groundwater potential index maps were created in the present research utilizing the frequency ratio technique with remote sensing data, primary and secondary data, and GIS tools. Nine significant thematic layers regulating the groundwater recharge were mapped. The frequency ratio method was adopted for allocating rating (r) values to each class by computing spatial connections between dependent variables (springs and wells) and the independent variable (thematic layers). The weighted linear combination approach was used to combine the nine theme layers to determine possible groundwater zones. According to the study results, 39.23% of the current study includes low groundwater potential zones, 38.33% covers medium groundwater potential zones, and 22.44% covers high groundwater potential zones. The output of the present study was validated through the AUC method. The success and prediction rate AUC values suggest that the technique employed in this investigation was highly successful. Finally, the findings of this study demonstrated that the FR model might indeed be utilized successfully in the groundwater potentiality mapping.

References

1. Nampak H, Pradhan B, Abd Manap M (2014) Application of GIS based data driven evidential belief function model to predict groundwater potential zonation. J Hydrol 513:283–300
2. Chen W, Li H, Hou E, Wang S, Wang G, Panahi M, Niu C (2018) GIS-based groundwater potential analysis using novel ensemble weights-of-evidence with logistic regression and functional tree models. Sci Total Environ 634:853–867
3. Arulbalaji P, Padmalal D, Sreelash K (2019) GIS and AHP techniques based delineation of groundwater potential zones: a case study from southern Western Ghats, India. Sci Rep 9(1):1–17
4. Das S (2019) Comparison among influencing factor, frequency ratio, and analytical hierarchy process techniques for groundwater potential zonation in Vaitarna basin, Maharashtra, India. Groundwater Sustain Dev 8:617–629
5. Ahmed N, Hoque MAA, Pradhan B (2021) Spatio-temporal assessment of groundwater potential zone in the drought-prone area of Bangladesh using GIS-based bivariate models. Nat Resour Res. https://doi.org/10.1007/s11053-021-09870-0
6. Mengistu HA, Demlie MB, Abiye TA (2019) Review: groundwater resource potential and status of groundwater resource development in Ethiopia. Hydrogeol J 27:1051–1065. https://doi.org/10.1007/s10040-019-01928-x
7. Semu M (2012) Agricultural use of groundwater in Ethiopia: assessment of potential and analysis of economics, policies, constraints and opportunities. IWMI, Addis Ababa Ethiopia
8. Berhanu KG, Hatiye SD (2020) Identification of groundwater potential zones using proxy data: case study of Megech watershed, Ethiopia. J Hydrol Reg Stud 28:100676. https://doi.org/10.1016/J.EJRH.2020.100676
9. Moges DM, Bhat HG, Thrivikramji KP (2019) Investigation of groundwater resources in highland Ethiopia using a geospatial technology. Model Earth Syst Environ 5:1333–1345. https://doi.org/10.1007/s40808-019-00603-0
10. Ahmad I, Dar MA, Teka AH, Teshome M, Andualem TG, Teshome A, Shafi T (2020) GIS and fuzzy logic techniques-based demarcation of groundwater potential zones: a case study from Jemma River basin, Ethiopia. J Afr Earth Sci 169:103860. https://doi.org/10.1016/J.JAFREARSCI.2020.103860
11. Tolche AD (2021) Groundwater potential mapping using geospatial techniques: a case study of Dhungeta-Ramis sub-basin, Ethiopia. Geol Ecol Landscapes 5(1):65–80. https://doi.org/10.1080/24749508.2020.1728882
12. MacDonald AM, Bonsor HC, Dochartaigh BÉÓ, Taylor RG (2012) Quantitative maps of groundwater resources in Africa. Environ Res Lett 7(2):024009. British Geological Survey Groundwater Programme Internal Report Ir/10/103. https://doi.org/10.1088/1748-9326/7/2/024009
13. Das S, Pardeshi SD (2018) Morphometric analysis of Vaitarna and Ulhas river basins, Maharashtra, India: using geospatial techniques. Appl Water Sci 8:158. https://doi.org/10.1007/s13201-018-0801-z
14. Kumar T, Gautam AK, Kumar T (2014) Appraising the accuracy of GIS-based multi-criteria decision making technique for delineation of groundwater potential zones. Water Resour Manag 28(13):4449–4466. https://doi.org/10.1007/s11269-014-0663-6
15. Al-Shabeeb AA, Al-Adamat R, Al-Fugara A, Al-Amoush H, Al-Ayyash S (2018) Delineating groundwater potential zones within the Azraq basin of central Jordan using multi-criteria GIS analysis. Groundwater Sustain Dev 7:82–90. https://doi.org/10.1016/j.gsd.2018.03.011
16. Senapati U, Das TK (2021) Assessment of basin-scale groundwater potentiality mapping in drought-prone upper Dwarakeswar River basin, West Bengal, India, using GIS-based AHP techniques. Arab J Geosci 14:960. https://doi.org/10.1007/s12517-021-07316-8
17. Muralitharan J, Palanivel K (2015) Groundwater targeting using remote sensing, geographical information system and analytical hierarchy process method in hard rock aquifer system, Karur district, Tamil Nadu, India. Earth Sci Inf 8:827–842. https://doi.org/10.1007/s12145-015-0213-7

18. Mohammadi-Behzad HR, Charchi A, Kalantari N, Nejad AM, Vardanjani HK (2018) Delineation of groundwater potential zones using remote sensing (RS), geographical information system (GIS) and analytic hierarchy process (AHP) techniques: a case study in the Leylia–Keynow watershed, southwest of Iran. Carbonates Evaporites 34(4):1307–1319. https://doi.org/10.1007/S13146-018-0420-7

19. Muniraj K, Jesudhas CJ, Chinnasamy A (2020) Delineating the groundwater potential zone in Tirunelveli Taluk, South Tamil Nadu, India, using remote sensing, geographical information system (GIS) and analytic hierarchy process (AHP) techniques. Proc Natl Acad Sci India Sect A Phys Sci 90(4):661–676. https://doi.org/10.1007/S40010-019-00608-5

20. Andualem TG, Demeke GG (2019) Groundwater potential assessment using GIS and remote sensing: a case study of Guna tana landscape, upper blue Nile Basin, Ethiopia. J Hydrol Reg Stud 24:100610. https://doi.org/10.1016/J.EJRH.2019.100610

21. Pourtaghi Z, Pourghasemi HR (2014) GIS-based groundwater spring potential assessment and mapping in the Birjand Township, southern Khorasan Province, Iran. Hydrogeology 22:643–662. https://doi.org/10.1007/s10040-013-1089-6

22. Razandi Y, Pourghasemi HR, Neisani NS, Rahmati O (2015) Application of analytical hierarchy process, frequency ratio, and certainty factor models for groundwater potential mapping using GIS. Earth Sci Inf 8(4):867–883. https://doi.org/10.1007/s12145-015-0220-8

23. Jothibasu A, Anbazhagan S (2016) Modeling groundwater probability index in Ponnaiyar River basin of South India using analytic hierarchy process model. Earth Syst Environ 2:109. https://doi.org/10.1007/s40808-016-0174

24. Naghibi A, Pourghasemi HR (2015) A comparative assessment between three machine learning models and their performance comparison by bivariate and multivariate statistical methods for groundwater potential mapping in Iran. Water Resour Manag 29(14):5217–5236. https://doi.org/10.1007/s11269-015-1114-8

25. Zabihi M, Pourghasemi HR, Pourtaghi ZS, Behzadfar M (2016) GIS-based multivariate adaptive regression spline and random forest models for groundwater potential mapping in Iran. Environ Earth Sci 75:665. https://doi.org/10.1007/s12665-016-5424-9

26. Davoodi MD, Rezaei M, Pourghasemi HR, Pourtaghi ZS, Pradhan B (2015) Groundwater spring potential mapping using bivariate statistical model and GIS in the Taleghan watershed Iran Arab. J Geosci 8:913–929. https://doi.org/10.1007/s12517-013-1161-5

27. Manap MA, Nampak H, Pradhan B, Lee S, Sulaiman WNA, Ramli MF (2012) Application of probabilistic-based frequency ratio model in groundwater potential mapping using remote sensing data and GIS. Arab J Geosci 7(2):711–724. https://doi.org/10.1007/S12517-012-0795-Z

28. Guru B, Seshan K, Bera S (2017) Frequency ratio model for groundwater potential mapping and its sustainable management in cold desert, India. J King Saud Univ Sci 29(3):333–347. https://doi.org/10.1016/J.JKSUS.2016.08.003

29. Nejad SG, Falah F, Daneshfar M, Haghizadeh A, Rahmati O (2017) Delineation of groundwater potential zones using remote sensing and GIS-based data-driven models. Geocarto Int 32(2):167–187

30. Sahoo S, Munusamy SB, Dhar A, Kar A, Ram P (2017) Appraising the accuracy of multi-class frequency ratio and weights of evidence method for delineation of regional groundwater potential zones in canal command system. Water Resour Manag 31(14):4399–4413

31. Jothimani M, Abebe A, Dawit Z (2020) Mapping of soil erosion-prone sub-watersheds through drainage morphometric analysis and weighted sum approach: a case study of the Kulfo River basin, Rift valley, Arba Minch, Southern Ethiopia. Model Earth Syst Environ 6:2377–2389. https://doi.org/10.1007/s40808-020-00820-y

32. Jothimani M, Abebe A, Duraisamy R (2021) Drainage morphometric analysis of Shope watershed, Rift Valley, Ethiopia: remote sensing and GIS-based approach. IOP Conf Ser Earth Environ Sci 796(1):012009. https://doi.org/10.1088/1755-1315/796/1/012009

33. Ayazi MH, Pirasteh S, Arvin AKP, Pradhan B, Nikouravan B, Mansor S (2010) Disasters and risk reduction in groundwater: Zagros Mountain southwest Iran using geo-informatics techniques. Dis Adv 3(1):51–57

34. Anbazhagan S, Balamurugan G, Biswal TK (2011) Remote sensing in delineating deep fracture aquifer zones. In: Anbazhagan S, Subramanian SK, Yang X (eds) Geoinformatics in applied geomorphology. Taylor and Francis, CRC Press, pp 205–229
35. Prasad RK, Mondal NC, Banerjee P, Nandakumar MV, Singh VS (2008) Deciphering potential groundwater zone in hard rock through the application of GIS. Environ Geol 55(3):467–475
36. Maidment D (2002) ArcHydro GIS for water resources. ESRI Press, Redlands, CA
37. Bhattacharya AK (2010) Artificial ground water recharge with a special reference to India. Int J Res Rev Appl Sci 4:214–221
38. Das S, Gupta A, Ghosh S (2017) Exploring groundwater potential zones using MIF technique in semi-arid region: a case study of Hingoli district, Maharashtra. Spat Inf Res 25(6):749–756. https://doi.org/10.1007/s41324-017-0144-0
39. Lone MS, Nagaraju D, Mahadavesamy G, Siddalingamurthy S (2013) Applications of GIS and remote sensing to delineate artificial recharge zones (DARZ) of groundwater in HD Kote taluk, Mysore district, Karnataka, India. Int J Remote Sens Geosci 2(3):92–97
40. Lillesand T, Kiefer RW, Chipman J (2007) Remote sensing and image interpretation. Wiley, Hoboken
41. Rajaveni SP, Brindha K, Elango L (2015) Geological and geomorphological controls on ground-water occurrence in a hard rock region. Appl Water Sci 7(3):1377–1389. https://doi.org/10.1007/s13201-015-0327-6
42. Food and Agriculture Organization (FAO) (1997) The digital soil and terrain database of East Africa (SEA), via delle Terme di Caracalla, Rome, Italy
43. Sar N, Khan A, Chatterjee S (2015) Hydrologic delineation of ground water potential zones using geospatial technique for Keleghai river basin, India. Model Earth Syst Environ 1:25. https://doi.org/10.1007/s40808-015-0024-3
44. Teshome A, Halefom A, Ahmad I (2020) Fuzzy logic techniques and GIS-based delineation of groundwater potential zones: a case study of Anger river basin, Ethiopia. Model Earth Syst Environ. https://doi.org/10.1007/s40808-020-01035-x
45. Bonham-Carter GF (1994) Geographic information systems for geoscientists, modeling with GIS. Pergamon Press, Oxford
46. Pradhan B (2013) A comparative study on the predictive ability of the decision tree, support vector machine and neuro-fuzzy models in landslide susceptibility mapping using GIS. Comput Geosci 51:350–365